Progress In Electromagnetics Research C, Vol. 23, 1–14, 2011

QUADRI-FOLDED SUBSTRATE INTEGRATED WAVEGUIDE CAVITY AND ITS MINIATURIZED BANDPASS FILTER APPLICATIONS

C. A. Zhang, Y. J. Cheng*, and Y. Fan

EHF Key Lab of Fundamental Science, School of Electronic Engineering, University of Electronic Science and Technology of China, Xiyuan Road 2006, Chengdu 611731, P. R. China

Abstract—In this paper, a quadri-folded substrate integrated waveguide (QFSIW) resonant cavity is proposed and investigated for the first time, which is able to reduce the circuit size by 89% compared with the conventional substrate integrated waveguide (SIW) resonant cavity. It has a two-layer configuration and a C-type coupling slot etched on the middle conductor layer. As an example, such a miniaturized resonant cavity is employed in the design of a four-order S-band SIW bandpass filter with the Chebyshev response. Negative couplings are used between two adjacent SIW resonant cavities, which don't influence the whole transmission characteristic of the filter. Experimental results are in good agreement with those from simulations.

1. INTRODUCTION

Substrate integrated waveguide (SIW) has been proposed and used widely in the design of microwave and millimeter wave circuit since its inception. It keeps the merits of planar transmission lines and rectangular waveguides (RWs). As such, a number of passive and active devices have been proposed and realized based on the SIW techniques [1–6].

As well known, waveguide-based and SIW-based filters usually have better performance than other planar counterpart structures. However, their use may be restricted because of the relative large physical dimension. To overcome such a drawback, some miniaturized

Received 24 May 2011, Accepted 11 July 2011, Scheduled 22 July 2011
* Corresponding author: Yu Jian Cheng (yjcheng@emfield.org).

resonant cavity structures were proposed and investigated. For example, a double-folded RW resonant cavity was introduced in 2004 [7]. It is a two-layer waveguide resonant cavity with L-type slot in the middle conductor layer, thus it can reduce the circuit area by 75% compared with the conventional RW resonant cavity. Some researchers made efforts to reduce the size of SIW resonant cavity as well [8–13]. Nevertheless, there is still room for improvement.

In this paper, a new type of quadri-folded SIW (QFSIW) resonant cavity is introduced to reduce the circuit area of conventional SIW resonant cavity to be 89%. Conductor-backed sandwiched CPW is employed as the feeding structure to transmit power from microstrip line into the QFSIW resonant cavity. After that, an S-band four-cavity filter is developed and fabricated based on the proposed miniaturized SIW resonant cavity. The center frequency is 3.2 GHz and the average insertion loss within the in-band is measured to be 1.6 dB. Detailed design process is introduced to synthesize such a miniaturized SIW bandpass filter with the required specifications.

2. QUADRIFOLDED SUBSTRATE INTEGRATED WAVEGUIDE CAVITY

2.1. Configuration

The E-field distribution of SIW resonant cavity is similar to that of RW resonant cavity when it operates within the dominant mode zone. Therefore, a single-layer SIW resonant cavity can be folded to be a double-layer structure with a slot etched on the middle conductor layer to couple the up-layer and down-layer together. Slots with different shape reduce different circuit area.

Here we designed a special slot, i.e., C-type slot, etched on the middle conductor layer as shown in Figs. 1 and 2. It can be referenced to be folded four times. The up cavity and down cavity are grouped through this C-type slot as a whole. On the other hand, it introduces additional capacitance effect and makes an approximately three times increase in the equivalent width of the QFSIW resonant cavity. As such, the equivalent area of our structure can be expanded by about nine times. The capacitance value can be controlled by the location and the size of C-type slot. The increase of capacitance leads to the decrease of resonant frequency. Therefore, when the slot becomes shorter or wider, the resonant frequency will increase. When slot moves away from the edge, the same result will be concluded.

However, the fabrication limit will restrict the compression rate. Here, its resonant frequency can be determined by (1) when it operates

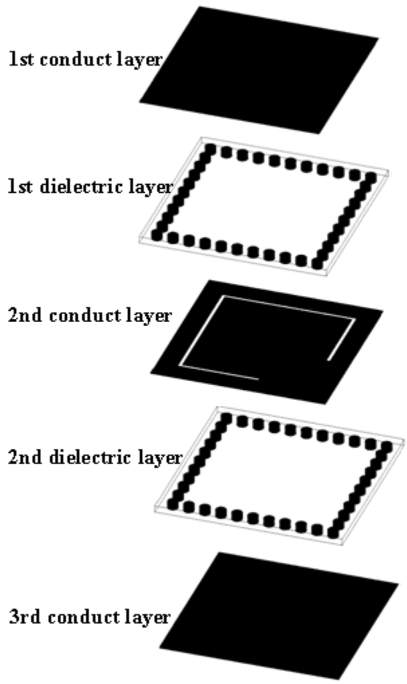

Figure 1. Configuration of the proposed QFSIW resonant cavity.

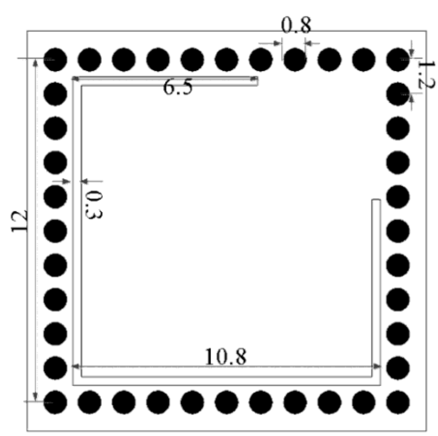

Figure 2. Dimension of the proposed QFSIW resonant cavity. (unit: mm).

with the dominant mode.

$$f_0 = \frac{c_0}{6 \times \sqrt{\varepsilon_r}} \sqrt{\frac{1}{a_{eff}^2} + \frac{1}{l_{eff}^2}} \tag{1}$$

where

$$\begin{aligned} a_{eff} &= a - \frac{d^2}{0.95p} \\ l_{eff} &= l - \frac{d^2}{0.95p} \end{aligned}$$

In (1), ε_r is the relative permittivity of substrate, c_0 represents the speed of light in a vacuum, a and l are the width and length of SIW cavity respectively, and d and p are the diameter of metallized via-holes and center-to-center pitch between two adjacent via-holes. Here, the size of conventional SIW resonant cavity can be greatly reduced by 89%.

The simulated E-field distribution within such a QFSIW resonant cavity is shown in Fig. 3. The E-fields distributed in the up-layer and down-layer is the same. Different from the conventional single-layer SIW resonant cavity, the maximum E-field in the QFSIW resonant cavity is concentrated at the slot region, and not at the central area. Besides, the E-field at the opening of C-type slot is weak. Our configuration has a smaller Q value compared with that of a conventional single-layer resonator. It is unavoidable because the

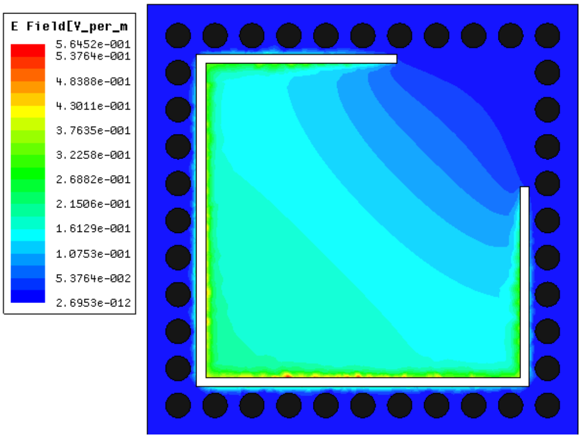

Figure 3. Electric field distribution within the proposed QFSIW resonant cavity.

resonator is folded four times. As such, loss will be higher than that of the conventional one.

2.2. Experiment

To verify our theory, the proper transition structure between the $50\,\Omega$ microstrip line and the QFSIW resonant cavity should be designed convenient for experiment. The microstrip line is converted into the conductor-backed sandwiched CPW at first. Then, the CPW is connected with C-type slot directly as shown in Fig. 4.

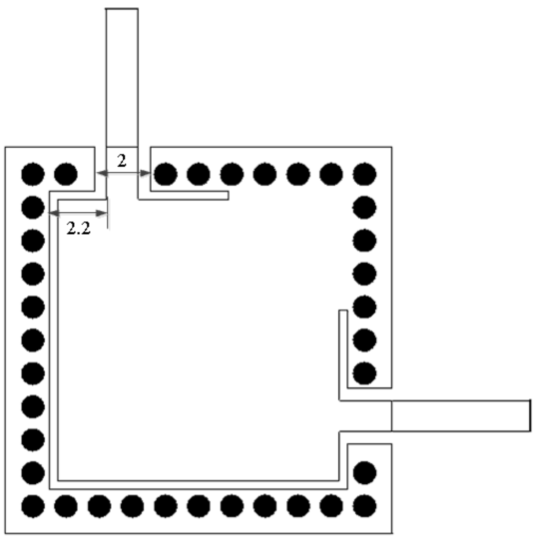

Figure 4. Configuration of the proposed QFSIW resonant cavity with transition. (unit: mm).

This prototype is fabricated on Taconic RF35 substrate with the relative permittivity of 3.5 and the height of 0.508 mm as shown in Fig. 5. Its $\tan\delta$ is 0.0018. As shown in Fig. 6, the resonant frequency is measured to be 3.2 GHz with $12\times12\,\mathrm{mm}^2$ area. The measured results and the simulated results are in good agreement. A conventional SIW resonant cavity with the same resonant frequency needs the circuit area of $36\times36\,\mathrm{mm}^2$. It can be found that the QFSIW resonant cavity is much smaller than its conventional SIW resonant cavity counterpart.

Table 1 lists the comparison results among different compact SIW resonant cavities as described in [14]. It is demonstrated that our configuration and the double folded half mode substrate integrated waveguide (DFHMSIW) resonant cavity are the two

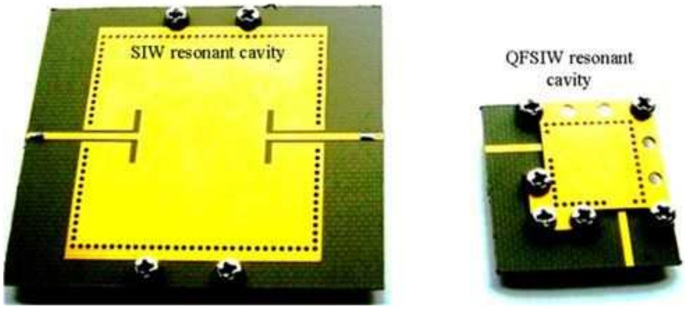

Figure 5. Photographs of the fabricated SIW resonant cavity and QFSIW resonant cavity at the same resonant frequency.

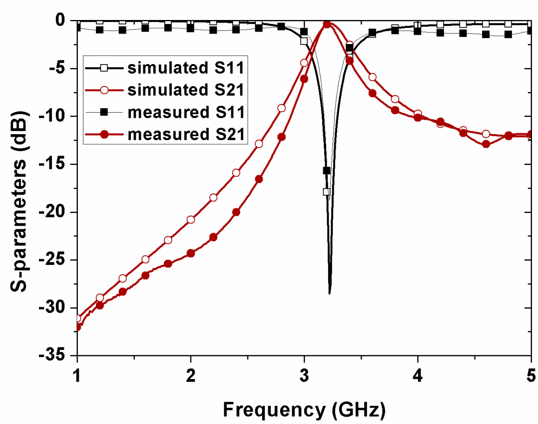

Figure 6. Simulated and measured results for the proposed QFSIW resonant cavity.

Table 1. Comparison among different SIW cavities.

The type of cavity	Reduced circuit area compared with SIW cavity
HMSIW in [15]	50%
DFSIW in [13]	75%
FHMSIW in [16]	Nearly 75%
DFHMSIW in [14]	Nearly 87%
QFSIW	89%

smallest structures. Although the sizes of DFHMSIW resonant cavity and QFSIW resonant cavity are almost the same, the QFSIW resonant cavity is more excellence in some performance, especially for low loss. The reason is that the QFSIW resonant cavity has closed structure to avoid the radiation leakage and unwanted coupling.

3. QFSIW FILTER DESIGN

3.1. Design Process

Now, the proposed QFSIW cavity will be employed to construct a miniaturized bandpass filter. Detailed design process will be introduced as follows.

3.1.1. External Coupling

External Coupling Q_e is one of the most important indexes in the filter design. It decides the center frequency, bandwidth and also controls the insertion loss in the passband. In our design, it can be effectively determined by the location of feeding pointing as shown in Fig. 7.

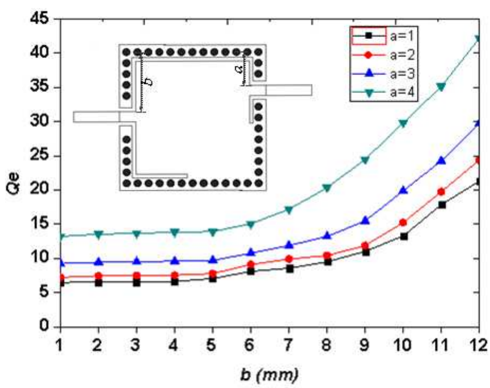

Figure 7. Relationship between the location of feeding and Q_e.

Q_e can be calculated by [17]:

$$Q_e = \frac{2f_0}{\Delta f_{3\,\mathrm{dB}}} \tag{2}$$

where f_0 is the resonant frequency and $\Delta f_{3\,\mathrm{dB}}$ is the 3 dB bandwidth.

3.1.2. Internal Coupling

The magnetic coupling is usually employed in the design of conventional SIW bandpass filter. The internal coupling intensity is mainly controlled by the width of the inductive window. But in this paper, it is difficult to achieve a positive coupling between adjacent QFSIW resonant cavities. As such, the electric coupling is employed considering its special configuration. The coupling ratio can be determined by the location of coupling structure as shown in Fig. 8. In Fig. 9, two split mode frequencies (resonant peaks) are observable. These two split frequencies labeled as f_1 for the first peak and f_2 for the second peak. The coupling coefficient between two adjacent resonators

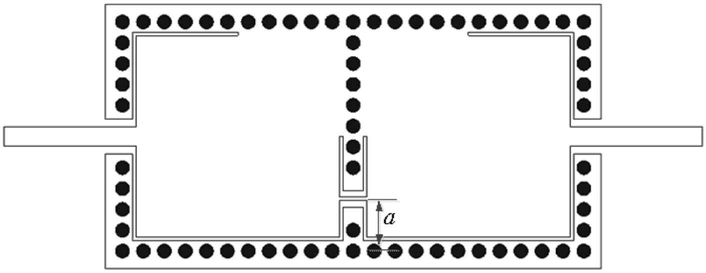

Figure 8. Internal coupling between QFSIW resonant cavities.

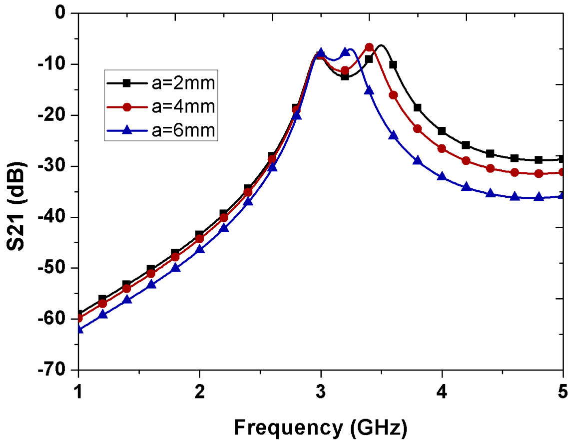

Figure 9. Frequency response of the proposed coupling structure between two QFSIW resonant cavities.

can be calculated by [17]:

$$k = \frac{f_1^2 - f_2^2}{f_1^2 + f_2^2} \tag{3}$$

Larger a makes such two resonant peaks closer. It suggests that the electric coupling becomes weaker with the increase of a. The relationship between coupling coefficient k and the value of a is shown in Fig. 10.

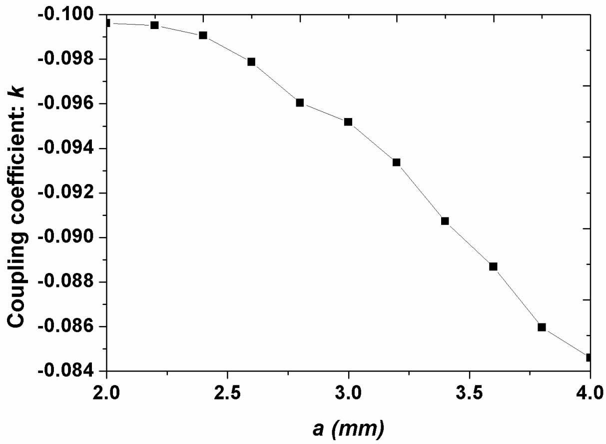

Figure 10. Relationship between k and a.

3.1.3. Circuit Synthesis

Here, a four-order bandpass QFSIW filter is constructed by four cascaded QFSIW resonant cavities, which has the electrical coupling between adjacent cavities. With the desired coupling coefficient and external quality factor Q_e, the coupled-resonator filter can be designed as described in [17].

The coupling coefficients k and the external quality Q_e can be extracted as the following formula:

$$\begin{aligned} Q_e &= \frac{1}{FBW \times M_{S1}^2} \\ k_{ij} &= FBW \times M_{ij} \\ FBW &= \frac{BW}{f_0} \end{aligned} \tag{4}$$

where f_0 is the center frequency, BW is bandwidth, and M_{ij} is the element in coupling matrix. The designed filter should satisfy the specification: $f_0 = 3.2\,\text{GHz}$, $BW = 300\,\text{MHz}$, and return loss in-band is better than 25 dB. Thus the required coupling matrix is calculated to:

$$M = \begin{pmatrix} & S & 1 & 2 & 3 & 4 & L \\ S & 0 & 1.1515 & 0 & 0 & 0 & 0 \\ 1 & 1.1515 & 0 & -1.0401 & 0 & 0 & 0 \\ 2 & 0 & -1.0401 & 0 & -0.7710 & 0 & 0 \\ 3 & 0 & 0 & -0.7710 & 0 & -1.0401 & 0 \\ 4 & 0 & 0 & 0 & -1.0401 & 0 & 1.1515 \\ L & 0 & 0 & 0 & 0 & 1.1515 & 0 \end{pmatrix} \quad (5)$$

Thus, the required parameters of the proposed filter are: $k_{12} = -0.0975$, $k_{23} = -0.0723$, $k_{34} = -0.0975$, and $Q_e = 8.04$. The

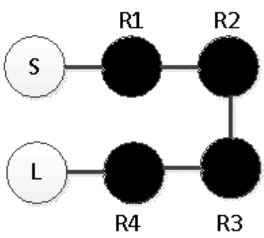

Figure 11. Schematic topology of the proposed miniaturized filter.

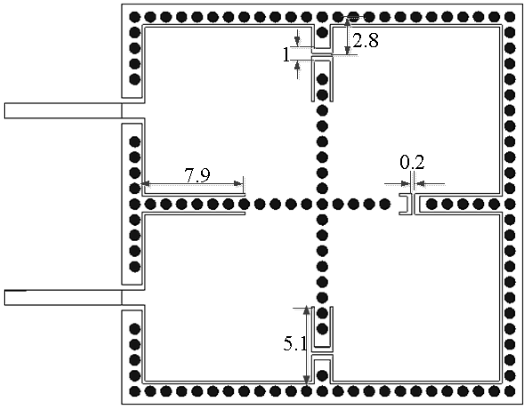

Figure 12. Geometric configuration of the proposed miniaturized filter. (unit: mm).

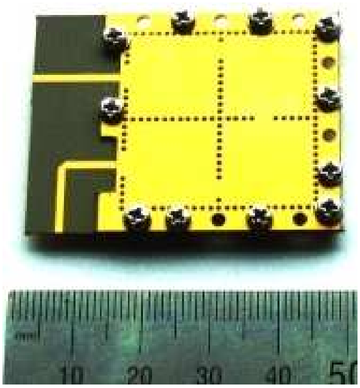

Figure 13. Photograph of the fabricated miniaturized filter.

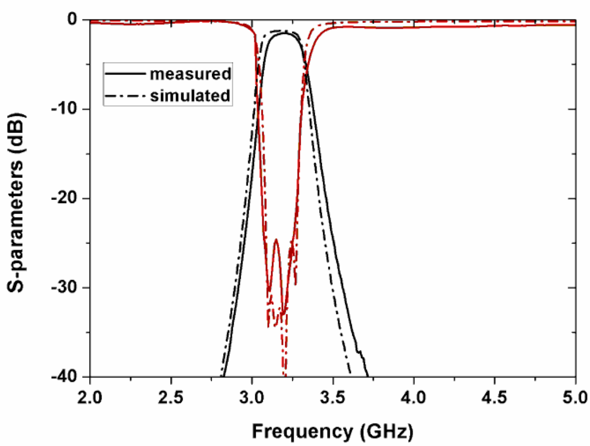

Figure 14. Measured and simulated results of the fabricated miniaturized filter.

schematic topology of the proposed miniaturized filter is shown in Fig. 11, and its geometric configuration is presented in Fig. 12.

3.2. Experiments

The four-cavity Chebyshev filter based on QFSIW resonant cavities is simulated and optimized by HFSS software and fabricated by standard PCB process as shown in Fig. 13. The used substrate is also Taconic RF-35 ($h = 0.508\,\text{mm}$, $\varepsilon_r = 3.5$, $\tan\delta = 0.0018$). The network analyzer is used to measure the filter. Simulated and measured results are shown in Fig. 14 and reasonable agreement is obtained between them. The measured in-band return loss is better than 25 dB, and the insertion loss is approximately 1.6 dB.

4. CONCLUSION

A QFSIW resonant is proposed and studied in detail, which can reduce the circuit area of conventional SIW resonant cavity by 89%. Therefore, it is suitable in the design of miniaturization circuit, such as filter. A QFSIW with proper feeding structure and a corresponding bandpass miniaturized filter are fabricated by the low cost PCB process. The results of experiment and simulation are in good agreement.

ACKNOWLEDGMENT

This work is supported in part by the National Natural Science Foundation of China (NSFC) under grant 61001028, in part by Research Fund for the Doctoral Program of Higher Education of China (RFDP) under grant 20100185110014, and in part by the Fundamental Research Funds for the Central Universities under grant ZYGX2010J019.

REFERENCES

1. Uchimura, H., T. Takenoshita, and M. Fuji, "Development of 'a laminated waveguide'," *IEEE Transactions on Microwave Theory and Techniques*, Vol. 46, No. 9, 2438–2443, Sep. 1998.
2. Hirokawa, J. and M. Ando, "Efficiency of 76-GHz post-wall waveguide-fed parallel-plate slot arrays," *IEEE Trans. Antennas Propag.*, Vol. 48, No. 11, 1742–1745, Nov. 2000.
3. Hong, W., K. Wu, H. J. Tang, J. X. Chen, P. Chen, Y. J. Cheng, and J. F. Xu, "SIW-liked guided wave structure and application," *IEICE Transaction on Electronic*, Vol. E92.C, No. 9, 1111–1123, Sep. 2009.
4. Cheng, Y. J., W. Hong, and K. Wu, "Broadband self-compensating phase shifter combining delay line and equal-length unequal-width phaser," *IEEE Transactions on Microwave Theory and Techniques*, Vol. 58, No. 1, 203–210, Jan. 2010.
5. Cheng, Y. J., W. Hong, K. Wu, and Y. Fan, "Millimeter-wave substrate integrated waveguide long slot leaky-wave antennas and

two-dimensional multibeam applications," *IEEE Trans. Antennas Propag.*, Vol. 59, No. 1, 40–47, Jan. 2011.

6. Cheng, Y. J., W. Hong, K. Wu, and Y. Fan, "A hybrid guided-wave structure of half mode substrate integrated waveguide and conductor-backed slotline and its application in directional couplers," *IEEE Microw. Wireless Compon. Lett.*, Vol. 21, No. 2, 65–67, Feb. 2011.
7. Hong, J. S., "Compact folded-waveguide resonators and filters," *IEE Proceedings Microwaves, Antennas and Propagation*, Vol. 153, 325–329, 2006.
8. Huang, T. Y., T. M. Shen, and B. J. Chen, "Design of miniaturized vertically stacked SIW filters in LTCC," *European Microwave Conference*, 413–416, 2009.
9. Wang, R., X. L. Zhou, and L. S. Wu, "A folded substrate integrated waveguide cavity filter using novel negative coupling," *Microwave and Optical Technology Letters*, Vol. 51, No. 3, 866–871, 2009.
10. Wang, R., L. S. Wu, and X. L. Zhou, "Compact folded substrate integrated waveguide cavities and bandpass filter," *Progress In Electromagnetics Research*, Vol. 84, 135–147, 2008.
11. Zhang, R. Q., Z. G. Wang, B. Yan, and R. M. Xu, "FSIW cavity filter and derivative FSIW cavity and its filters with LTCC technology," *Asia-Pacific Microwave Conference*, 1360–1363, 2009.
12. Che, W. Q., D. P. Wang, L. Xu, and C. X. Li, "Investigation on quality factor of substrate-integrated waveguide resonance cavity," *Microwave and Optical Technology Letters*, Vol. 49, No. 8, 2007–2010, Aug. 2007.
13. Chien, H. Y., T. M. Shen, T. Y. Huang, W. H. Wang, and R. B. Wu, "Miniaturized bandpass filters with double-folded substrate integrated waveguide resonators in LTCC," *IEEE Transactions on Microwave Theory and Techniques*, Vol. 57, No. 7, 1774–1782, 2009.
14. Hong, W. and K. Gong, "Miniaturization of substrate integrated bandpass filters," *Asia-Pacific Microwave Conference Proceedings (APMC)*, 247–250, 2010.
15. Gong, K., W. Hong, H. J. Tang, and J. X. Chen, "C-band bandpass filter based on half mode substrate integrated waveguide (HMSIW) cavities," *Asia-Pacific Microwave Conference*, 7–10, Dec. 2009.
16. Gong, K., W. Hong, J. Chen, H. Tang, D. Hou, and Y. Zhang,

"Novel compact bandpass filter based on folded half mode substrate integrated waveguide cavities," *Global Symposium on Millimeter Waves*, 14–16, Incheon, Apr. 2010.

17. Hong, J. S. and M. J. Lancaster, *Microstrip Filters for RF/Microwave Applications*, Chapter 8, 235–271, Wiley, New York, 2001.